

# Chapter 11

## Handling Membrane FEM Results

### 11.1 Surprising Stresses

#### 11.1.1 Effect of Poisson's Ratio

We consider a box-shaped steel bridge as shown in Figure 11.1. The box has two horizontal walls, at the top and bottom respectively, and two vertical walls, one at each outer side. There are no inner vertical longitudinal webs in the bridge. The structure is a new bridge on an existing pier that had been used for a narrower structure. Therefore, the two bearings at each bridge end do not coincide with the vertical side walls of the box structure, but are in a position more inward. It makes the end diaphragm behave as a beam with a four-point loading as drawn in Figure 11.1. The diaphragm consists of three parts, two squares outside the bearings and one between the bearings which has a length over depth ratio of two. The outer vertical walls are schematized as vertical stiffeners at the ends of the diaphragm. These walls carry forces  $F$  to the two ends of the diaphragm. These point loads cause support reactions  $F$  in the bearings. In order to introduce these concentrated sup-

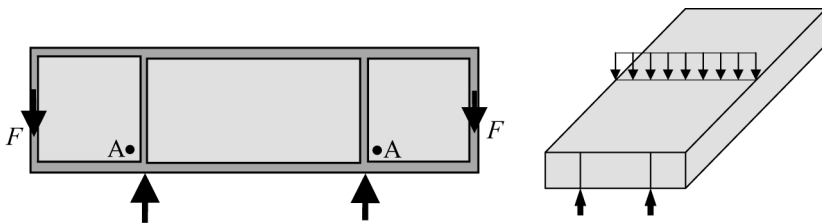


**Figure 11.1** End diaphragm of box-shaped bridge.

port reactions in the web of the diaphragm, two vertical stiffeners have been added at the position of the bearings. The diaphragm will bend such that the upper edge becomes longer and the lower edge shorter. Because of compatibility reasons, parts of the horizontal walls of the box will then participate in the transfer of the forces. In Figure 11.1 these parts have been modeled as horizontal stiffeners over the full length of the diaphragm, top and bottom.

Now we draw attention to the spots A in the diaphragm. The normal force in the vertical stiffener will be  $N_{\text{vert}} = -F$ . The normal force in the horizontal stiffener at that position will also be  $N_{\text{hor}} = -F$ . This result means that the strains are equal, to  $\epsilon$ , in the vertical and horizontal stiffeners at position A. The stress  $\sigma$  in the vertical stiffener is  $\sigma = E\epsilon$ . Because of compatibility the strains in the web material adjacent to the stiffener must be of the same size:  $\epsilon_{xx} = \epsilon_{yy} = \epsilon$ . The stress in the web plate must be calculated with Eq. (1.13):

$$\sigma_{yy} = \frac{E}{1 - \nu^2} (\epsilon_{yy} + \nu\epsilon_{xx}) = \frac{E}{1 - \nu} \epsilon \quad (11.1)$$

For Poisson's ratio  $\nu = 0.3$  we find a stress is  $\sigma_{yy} = E\epsilon_{yy}/0.7 = 1.43E\epsilon$ , 43% larger than the stress  $\sigma = E\epsilon$  in the adjacent stiffener with the same strain. Accounting for Poisson's ratio in this way can be important, particularly if buckling must be considered. The web is compressed, both in the horizontal and vertical direction.

### 11.1.2 Effect of Kink in Beam Flange

Now consider a clamped beam of I-section subjected to a point load at its free end, as shown in Figure 11.2. The cross-section of the beam consists of two flanges and a web. The width of the flanges and depth of the web are equal. The top flange is straight over the full length of the beam. The bottom flange is parallel to the top flange over about two-third of the beam counted from the clamped end, but then the height of the web decreases linearly to about half its height at the free end. As a result a kink occurs in the bottom flange. The subject of this Section is the distribution over the beam length of the bending stress  $\sigma$  in the connection line between the web and the bottom flange. Classic beam theory predicts  $\sigma = M/W$ , where  $M$  is the bending moment and  $W$  the section modulus. The bending moment  $M$  varies linearly over the length of the beam;  $W$  is constant between the clamped end and kink, and decreases in a nonlinear way to about one quarter of the constant value at the free end. So the expected stress distribution will

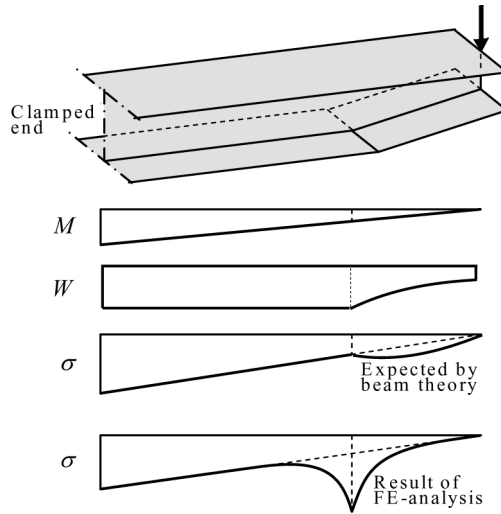


**Figure 11.2** Unexpected effect of kink in bottom flange.

be linear between the clamped edge and kink. Between the kink and free end the stress will be larger than for a constant  $W$ , but it will become zero at the free end.

As an alternative we can perform the calculation with the aid of a FEM program in which we choose membrane elements. We model the flanges by rectangular elements, say four over the half width. Choosing an aspect ratio of about two, we obtain the wanted number of elements over the length. For the web the same number of elements over length and depth is used. A sketch of the result to be expected from the FE analysis is included in Figure 11.2. It is completely different from the expectation on basis of the classical beam theory.

The explanation for the unexpected FEM result has to do with the fact that the classical beam solution is not admissible at the location of the kink. That solution predicts that a stress  $\sigma = M/W$  acts in the horizontal flange at the position of the kink and that the same stress acts in the inclined flange at that position. The two membrane forces meet each other at an angle, and therefore equilibrium can only exist if a third force in another direction acts in the same point to balance them. In reality there is no third force, so the membrane stresses in the bottom flange can be zero only at the location of the kink. In fact, there the I-section beam behaves as a T-section beam, consisting of the web and the top flange, shown in Figure 11.3. The section modulus reduces substantially, the neutral line shifts upward, and the bottom stress

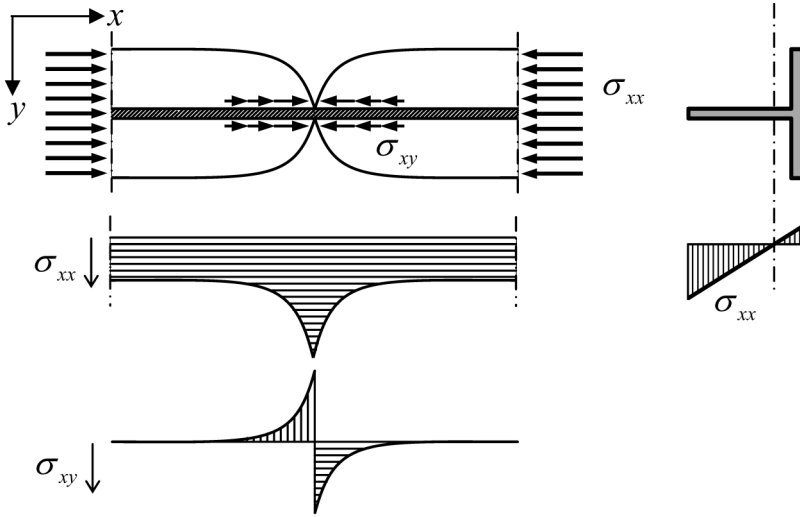


**Figure 11.3** Explanation of unexpected high bending stress.

increases. At some distance from the kink, the flange will contribute again. Shear stresses  $\sigma_{xy}$  between the web and each flange half must develop to obtain this effect. These shear stresses abruptly change sign and direction at the kink, and the bending stress  $\sigma_{xx}$  correspondingly decreases in two directions.

### ***FE analyses bring to light omissions in design***

FE analyses show stress concentrations where classic beam calculations suppose smooth stress distributions. Sometimes they bring merciless to light omissions in design.

Those who are familiar with bond stresses in a cracked reinforced concrete bar under tension will see a similarity. At a crack the reinforcement bar has to carry all the tensile force, and at some distance from the crack the concrete and bar carry the force together. A transition length occurs in which high bond shear stresses transfer part of the high tensile force in the crack to the concrete.

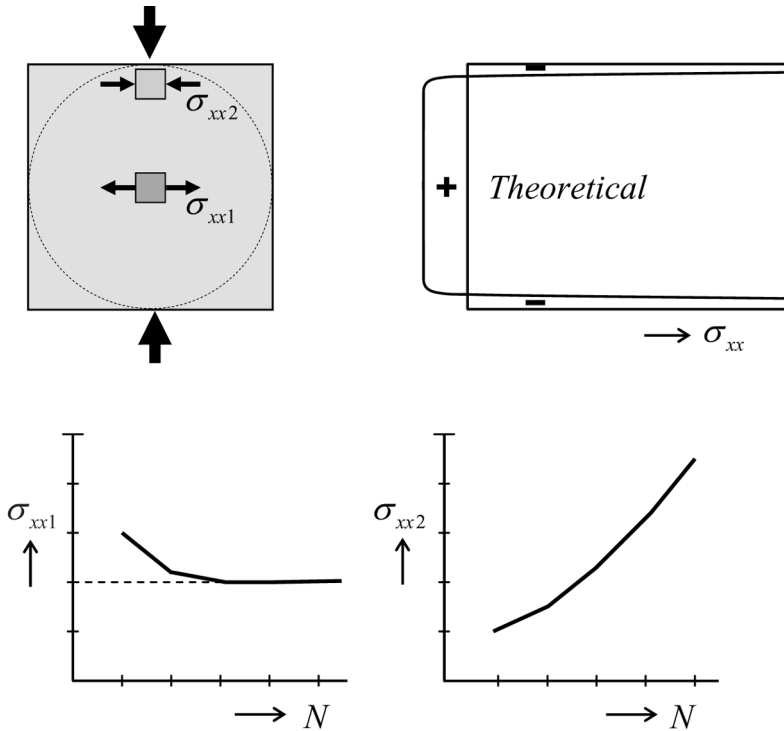


Figure 11.4 FE analyses do not converge in case of stress singularities.

## 11.2 Stress Singularities in FEM

In Section 6.2.2 we derived the stress state in the Brazilian splitting test. A cylindrical body is compressed by two opposed line loads. We found a constant horizontal tensile stress over the vertical plane of the cylinder and concentrated horizontal compressive point loads, one on the top and the other at the bottom, to balance the tensile stresses. In Figure 11.4 this test is simulated by a FE analysis. Instead of the circular cross-section, a square is chosen. The four corner areas outside the inner circle are relatively low-stress regions which hardly influence the stress state in the vertical plane of symmetry. The theoretical solution of the horizontal stress  $\sigma_{xx}$  is shown, and the stress is computed by FEM in two positions, point 1 at the top edge of the square and point 2 in the centre. The analysis is done for different mesh finesses, indicated by the number of elements  $N$  over the width and height of the cross-section. It is expected in a FE analysis that mesh refinement would

make the stress result converge to its final correct value. We notice that this is indeed the case for the stress at point 2, but not at point 1.

### *Lesson on singularities*

Convergence is obtained for stresses of finite value, but not at locations where the membrane plate theory predicts a singularity. Then no convergence will occur. The same is true for an infinitely large bending moment in plate bending, the subject of Chapter 14. There, too, mesh refinement does not make sense.

## 11.3 FEM-Supported Strut-and-Tie Modeling

If we have to design the reinforcement in concrete walls, it may be helpful for understanding force transfer to draw a Strut-and-Tie Model (STM). It is a truss-type model in which the load is represented by a set of well-chosen lumped forces, and the transfer to the supports occurs through a system of compressed struts and tensioned ties. In simple statically determinate problems the structural designer easily knows how to choose the strut and ties, but statically indeterminate structures may be puzzling, because more than one possibility exists. Figure 11.5 shows a simple example. A square silo is supported at the four corners and is subjected to a homogeneously distributed vertical load over the area of the walls. This load is due to own weight and possible friction of bulk material in the silo.

Each silo wall is a deep beam, of which the maximum bending moment occurs in the vertical line of symmetry at mid-span. The distribution of the horizontal stresses in this section must be known in order to design the reinforcement properly. The strut-and-tie model for an individual wall is simple, as appears from Figure 11.5. Green is compression, red is tension. In the line of symmetry at mid-span of the wall there is a compressive horizontal force and a tensile horizontal force of equal size. The product of the distance between these two forces times the value of the forces is the bending moment. The problem for the structural engineer is to make a fair guess about the distance, then calculate the tensile force and decide on the amount of horizontal reinforcement. Because the structure is highly statically indeterminate, the choice is hard to make. A FE analysis may help to make a good estimate.

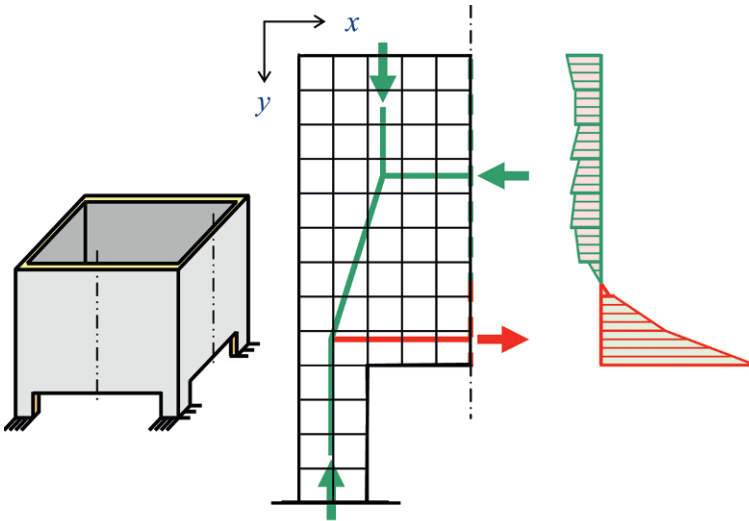


**Figure 11.5** FEM as support for Strut-and-Tie Model

We have analyzed the wall with a course mesh, which is appropriate. In fact the wall behaves as a deep beam, as discussed in Section 2.2.2. There we assumed that the wall has a distributed support over the full height of each vertical edge. The result for deep walls will be that the vertical support reaction is very much concentrated in the lower part of the edges. This distribution of the support reaction is close to the real support of the deep wall. The difference is then not significant. And for the rest, it anyhow is not relevant where the support occurs along the vertical edge. This does not influence the total beam moment which must be transferred in the vertical line of symmetry of the wall. The result of the FE analysis has been included in Figure 11.5. First, we see that the computed result agrees well with the theoretical expectation in Figure 2.13 for a short, tall wall. Second, the stress distribution along the line of symmetry nicely shows where we can choose the center of gravity of the tensile stresses and of the compressive stresses, which determine the positions of the horizontal tie and strut, respectively.

### *FE analysis as support for strut-and-tie modeling*

FE analysis supports the structural engineer in making strut-and-tie decisions. It helps positioning the reinforcement and determining lever arms.

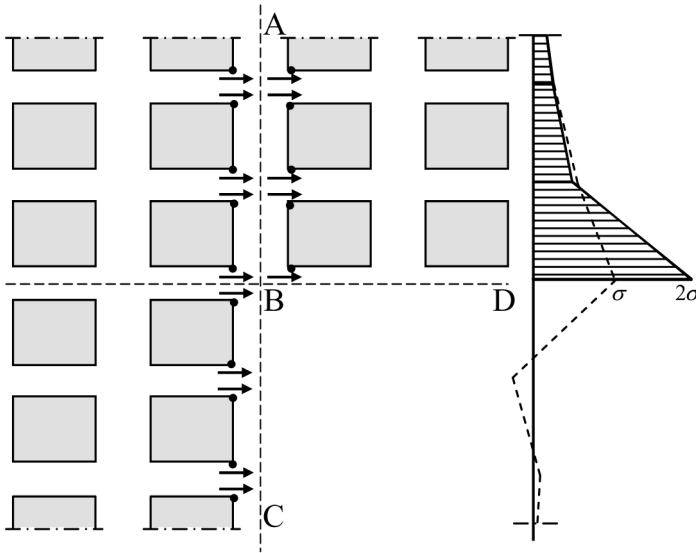


**Figure 11.6** Exploded view of elements around re-entrant corner.

## 11.4 Re-entrant Corner

The silo wall of Section 11.3 offers a good occasion to draw attention to a typical aspect which accompanies FE analyses for structures with a re-entrant corner. An example is displayed in Figure 11.6, which could be the corner between the column and the bottom edge of the wall. We have drawn in an exploded view rows and columns of rectangular elements around the corner. The re-entrant corner has edges BC and BD, so the corner is at node B. For ease of explanation it is assumed that the load is applied outside the considered part of the element mesh. We consider the vertical line which runs from node A over B to C, and focus on the horizontal forces at the nodes and the equilibrium of these forces. The two nodes between A and B can be seen as regular mesh nodes. Here four elements join together in a node and each element brings in an element force to the equilibrium equation for that node. The two forces coming from the left are more or less equal, and the same holds true for the two forces coming from the right. Equilibrium requires that the sum of the four forces is zero. The result is that the horizontal stresses in the four elements will be almost equal. An averaging procedure makes sense in such points. In corner node B a different situation exists. Now there are three element forces and they must sum to zero. The two left forces, more or less of equal size, must



balance those coming from the right. Therefore, the horizontal stress in the element to the right of node B is about twice the stress in the elements to the left of the node. If the stress to the left of the node is about  $\sigma$  in both elements, then it will be  $2\sigma$  to the right of the node. This latter size must be considered as the most realistic one. The average value is  $1.33\sigma$ , which is only two-third of the maximum stress  $2\sigma$ , the realistic one. Below corner B, only two element forces remain, which must be equal and opposite.

The stress state in the re-entrant corner is singular. In fact infinitely large shear stresses must occur in the horizontal line through corner node B to achieve that the stress  $2\sigma$  in the right plate part is spread over the two plate parts left of the vertical line. A disturbance occurs in the FE analysis which is still noticed in the edge nodes below the corner B. The stress distributions over sections just left and right of the vertical line through the corner node, sketched in Figure 11.6, visualize this. The dotted line represents the stresses to the left of the line ABC. It takes a couple of elements before the stress really is zero on the free edge BC. The explained phenomenon is inherent to the finite element method. The finer the element mesh, the smaller the region will be where the disturbance is seen. Similar effects are seen in plate bending near re-entrant corners. What we have explained here for plate forces, will occur there for plate moments.

#### ***Note on averaging procedures***

Averaging procedures can be misleading at re-entrant corners. The average value can be far less than the real maximum stress.

## **11.5 Tall Wall with Openings**

Multi-storey buildings often transmit wind loads to the base through shear walls of reinforced concrete. Shear walls may be positioned as end walls in building plans or as inner walls. At each storey an opening may occur; in end walls they allow for windows, and in inner walls they are necessary if a corridor crosses the wall, see Figure 11.7. We can view the tall wall with openings as a structure of two slender walls, left and right respectively, which are connected by horizontal cross-beams at each floor. Walls and beams together form one monolithic structure. If the shear wall is subjected

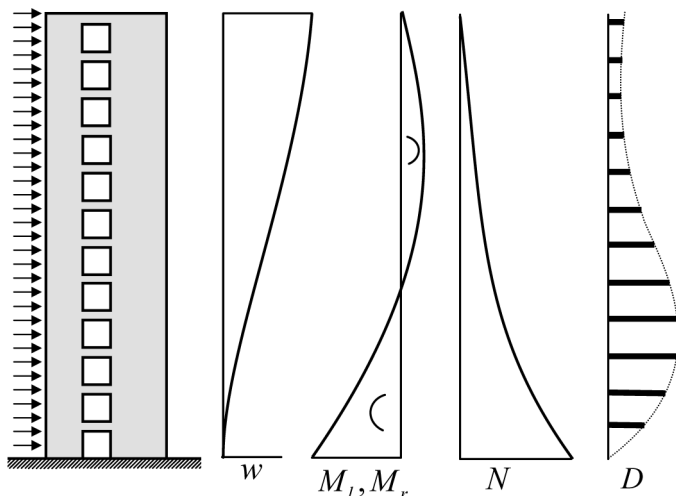


**Figure 11.7** Expected behaviour of tall wall with openings due to wind.

to wind load, the cross-beams will act as dowels, and the wall will deflect ( $w$ ) as sketched in Figure 11.7. The structural engineer is interested in the size of the transverse dowel forces (shear forces)  $D$  in the cross-beams, in order to detail the reinforcement in an adequate way. As a consequence of the dowel forces  $D$ , a tensile base force  $N$  will act in the left wall and a compressive base force  $N$  in the right. These normal forces carry part of the total wind moment at the base. The other part consists of bending moments in the left and right wall at the base,  $M_l$  and  $M_r$ , respectively. The total horizontal force due to the wind is the base shear, which is divided over the left and right wall  $V_l$  and  $V_r$  respectively. The base information is of interest to the structural designer in order to properly design the foundation. The expected diagrams for normal forces  $N$ , moments  $M$ , and beam dowel forces  $D$  are included in Figure 11.7. Of course, the analyst must superimpose the load due to self-weight.

In the 1960s and 1970s a lot of research on the force distribution in this type of structure was published on the basis of differential equations, among which contributions of Rosman [18] are well known. Today structural engineers will most probably apply FE analysis. In this section we comment on the FE modeling of this type of structure. We will do this in two ways: in Section 11.5.1 the focus is on modeling with membrane elements; in Section 11.5.2 it is on modeling as a frame structure.

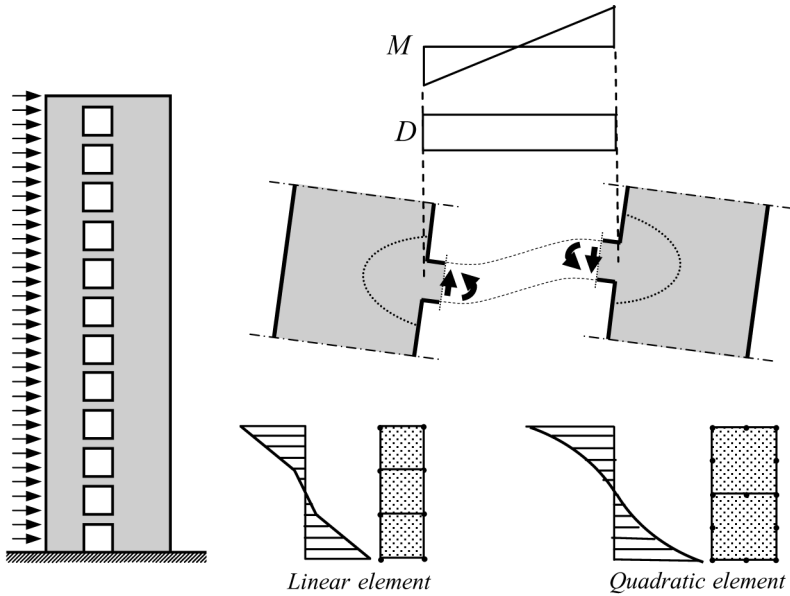


**Figure 11.8** Tall wall with row of openings.

### 11.5.1 Modeling with Membrane Elements

In Figure 11.8 we consider in more detail the force transfer in an individual cross-beam. The midpoint of beams is a point of counter-flexion. A constant shear force  $D$  occurs in the cross-beams, and the diagram for the bending moment  $M$  is linear with a zero value at mid-span.

At the connection between the cross-beams and the vertical walls, there will be high stress concentrations. Therefore, a sufficiently fine mesh must be chosen around beam-wall connections. Further away in the vertical walls a coarser mesh will be adequate. However, a coarse mesh is not really necessary in view of the speed and the mass storage of current computers. If the structural engineer chooses the membrane element with mid-side nodes (quadratic displacement) it suffices to use two elements over the depth of the cross-beam. For the element with only four corner nodes (linear displacements) three or more elements over the depth must be applied. Additionally, we recommend choosing the constant shear element because it performs better in situations where the element must reproduce bending states. The expected distribution of bending stresses in the cross-beams for linear and quadratic elements is included in Figure 11.8.

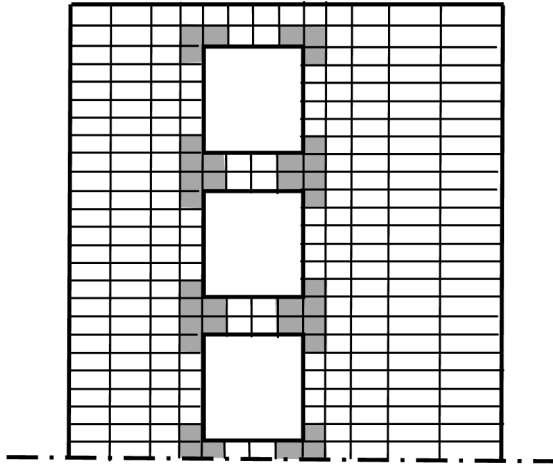


**Figure 11.9** The shaded elements will be seriously cracked.

Figure 11.9 shows the mesh with two elements over the depth. Because the largest moment occurs at the end of the cross-beam, and there is stress concentration at the connection, we expect substantial cracking. We can account for that by reducing the modulus of elasticity. Compared to the middle part of the cross-beams the actual stiffness might be halved. In Figure 11.9 we have marked these elements by shading. Reduction of the stiffness is important if the structure is sensitive to geometrical nonlinearity (second-order effects) and an increase of bending moments must be considered in stability checks.

### **11.5.2 Modeling as Frame**

Another way to investigate the force distribution in a tall wall with openings is to model the structure as a frame. In this case we must pay attention to a number of things. The frame consists of two vertical members (line elements), which coincide with the centre lines of the two slender walls. A horizontal member is placed in the centre line of each cross-beam. The modeling of the vertical members does not raise problems. The engineer must just make sure that the computer program accounts for deformation due to both normal forces and bending moments. Shear deformation need not be considered for slender walls. In the frame model, we introduce horizontal members with rigid end parts. The length of these rigid parts must be chosen

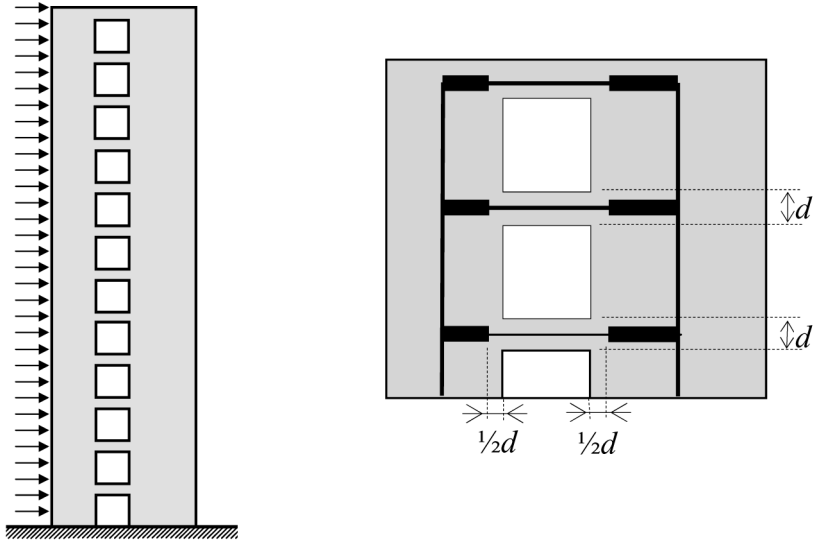


**Figure 11.10** Frame model of tall wall with openings.

with care. At first glance we may make the length half the width of the vertical walls, but then we make them too long. At the junction of the cross-beam and the walls, there will be deformation of the wall. Therefore, we recommend working with a fictitious length of the cross-beams larger than the real length. At each end the cross-beam may be extended by a length equal to the half depth of the beam, see Figure 11.10. So, the length of the rigid parts become smaller than the half width of the vertical walls.

Next to the choice of the length of the cross-beams, we must decide whether they behave as Bernoulli beams (flexural deformation only) or Timoshenko beams (flexural and shear deformation). Even after we increase the length of the cross-beam, it is still not slender. We must consider the half length of the beam, because of the zero value of the moment at mid-span. The half cross-beam is a cantilever beam with a point load at the end (point of counter-flexion), as discussed in Section 2.1.3. The length over depth ratio of the cantilever beam may become of the order of magnitude two and then, according to Eq. (2.57) stiffness reduction occurs. One can account for this either by using a program that accounts for shear deformation or by introducing a judiciously decreased bending stiffness.

Until now, we have assumed that the cross-beams have rectangular cross-section with the same width as the wall thickness. It is probably more com-

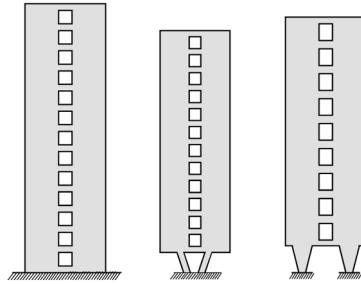


**Figure 11.11** Frame models easily include deviating support structures.

mon that floor slabs are fixed to the cross-beams. Then the engineer has to increase the bending stiffness of the cross-beam in the model, because of two reasons. The first reason is that the cross-beam becomes a T-shaped beam because the floor behaves as a flange of the cross-beam. It is not likely that this contribution is substantial. Participation of the floor as flange presupposes that a normal force can operate in the flange, however this requires a sufficient length to build up the normal force, and the half cross-beam is too short to obtain this. The other reason to include participation of the floor slab is the bending of the slab. It has to follow the curvatures of the cross-beam, so an effective slab width must be chosen, the bending stiffness of which is added to the bending stiffness of the cross-beam. To choose this effective slab width we could draw a line from the cross-beam centre with an angle of 45 degrees to the cross-beam. This implies, at the connection with the wall, a slab width at each side of the cross-beam of half the length of the beam.

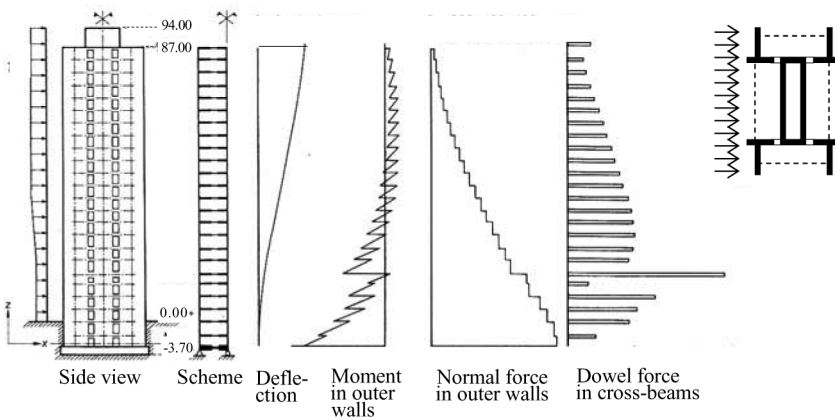


**Figure 11.12** Example of three coupled walls with two rows of openings.

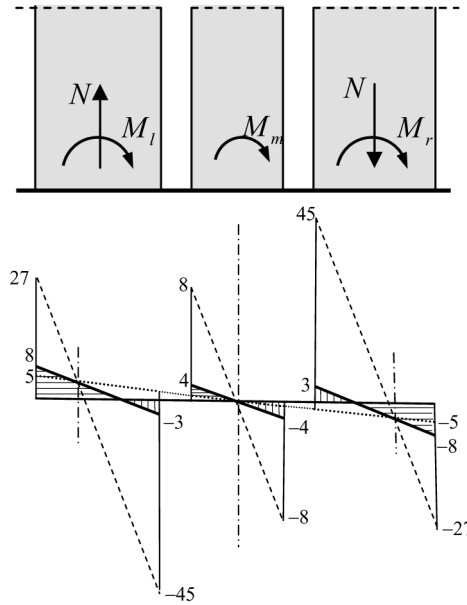


**Figure 11.13** Stress distribution in walls at base level. Dashed line for pin-connected cross-beams. Dotted lines for infinitely rigid cross-beams. Full line for real cross-beam stiffness.

Unlike the first, this second contribution to the beam bending stiffness may be substantial.

The frame method has a number of advantages. First, it provides results in a way structural engineers appreciate. The analysis leads to normal forces, shear forces and bending moments, for which code checking is familiar. Second, special supporting structures can easily be included in the model. Figure 11.11 demonstrates this. Third, it is easy to handle irregular structures with different storey heights and locally deviating cross-beam stiffness, and walls that are hard to model as a membrane plate fit easily in a frame model. Figure 11.12 shows an example. The building of about 90 meters height houses the administration offices of the government of a province in the Netherlands. The plan form is shown in the right-hand top part of the figure. The dashed lines are glass facades. In the plan, four T-shaped columns are connected with the corners of a central rectangular shaft. The connection of the columns to the shaft is by cross-beams at each floor level. A cross-beam of exceptional stiffness occurs at all four corners between the sixth and seventh storey. The building is subjected to wind at the long edge of the plan form.

The structure has been modeled as a system of three vertical walls and two rows of openings, as depicted in Figure 11.12. Because of symmetry, normal forces occur only in the two outer walls. The results of the analysis are included in Figure 11.12. At the position of the cross-beam with exceptional stiffness, there is a large dowel force  $D$ , which causes discontinuities in the bending moments and in the normal forces of the outer walls. Figure 11.13 displays the base stresses in the three walls. Note that the stress diagrams have the same gradient; this must hold because the three walls share the same deflection and therefore curvature. In the plot also the stresses are shown which would occur for two extreme situations, one in which the cross-beams are pin-connected and just act as trusses, and another in which the cross-sections are perfectly rigid such that all three walls act together as one wide beam, respectively. The actual maximum stress is about twice the stress for the ideal stiff case, however less than one-third of the pin-connected case.

## 11.6 Checking and Detailing

Commercial packages offer program features to check whether the design of structures is in accordance with codes of practice, or to dimension structural components. Here we just touch the subject to give an impression.

### 11.6.1 Steel

After a stress analysis has been performed for a steel structure, a so called unity check is made to confirm that the stress state in the structure is sufficient remote from the state of yielding. For that purpose the Von Mises stress  $\sigma_{VM}$  is calculated. In two-dimensional states this stress is

$$\sigma_{VM} = \sqrt{\sigma_1^2 + \sigma_2^2 - \sigma_1\sigma_2} \quad (11.2)$$

where  $\sigma_1$  and  $\sigma_2$  are principle stresses. The condition is that this stress is smaller than the yield stress  $\sigma_y$ :

$$\gamma_{\text{mat}} \sigma_{VM} \leq \sigma_y \quad (11.3)$$

Here  $\gamma_{\text{mat}}$  is the partial safety factor to be taken into consideration. Figure 11.14 visualizes the yield condition in the two-dimensional diagram for principal stresses. The actual combination of stresses must remain within the yield contour.



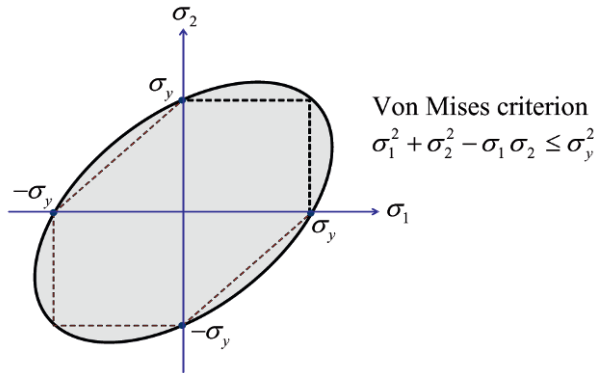


**Figure 11.14** Von Mises yield criterion. Dashed line Tresca.

### 11.6.2 Reinforced Concrete

For reinforced concrete structures, programs offer options to design the reinforcement automatically. We must solve a problem if we want to apply a two-way orthogonal reinforcement, because we have three membrane forces  $n_{xx}$ ,  $n_{yy}$  and  $n_{xy}$ . The subject will come up in detail in Chapter 16, but we will give a taste of the approach here. Consider a square panel with tensile normal membrane forces and a non-zero positive membrane shear force. In its most simple form the procedure is to replace the three membrane forces by two steel forces per unit length,  $n_{sx}$  and  $n_{sy}$ .

$$\begin{aligned} n_{sx} &= n_{xx} + n_{yx} \\ n_{sy} &= n_{yy} + n_{xy} \end{aligned} \tag{11.4}$$

and dimension the reinforcement in the  $x$ - and  $y$ -direction on the basis of these two forces. The idea behind this procedure is the assumption that the concrete is cracked. For the direction of the cracks only the shear membrane force  $n_{xy}$  is considered, which leads to principle forces in the direction of the diagonals of the panel, one tension and one compression respectively. The cracks are supposed to develop normal to the tensile principal force. This situation is shown in the top part of Figure 11.15. There the lower right triangular part represents concrete, and the upper left triangle shows the reinforcement bars. Equation (11.4) follows from the equilibrium conditions in the  $x$ - and  $y$ -direction of the concrete triangle. If the shear force has an opposite sign, the crack direction reverses. The relations in Eq. (11.4) still hold true if we use the absolute value of the shear forces, as follows from the

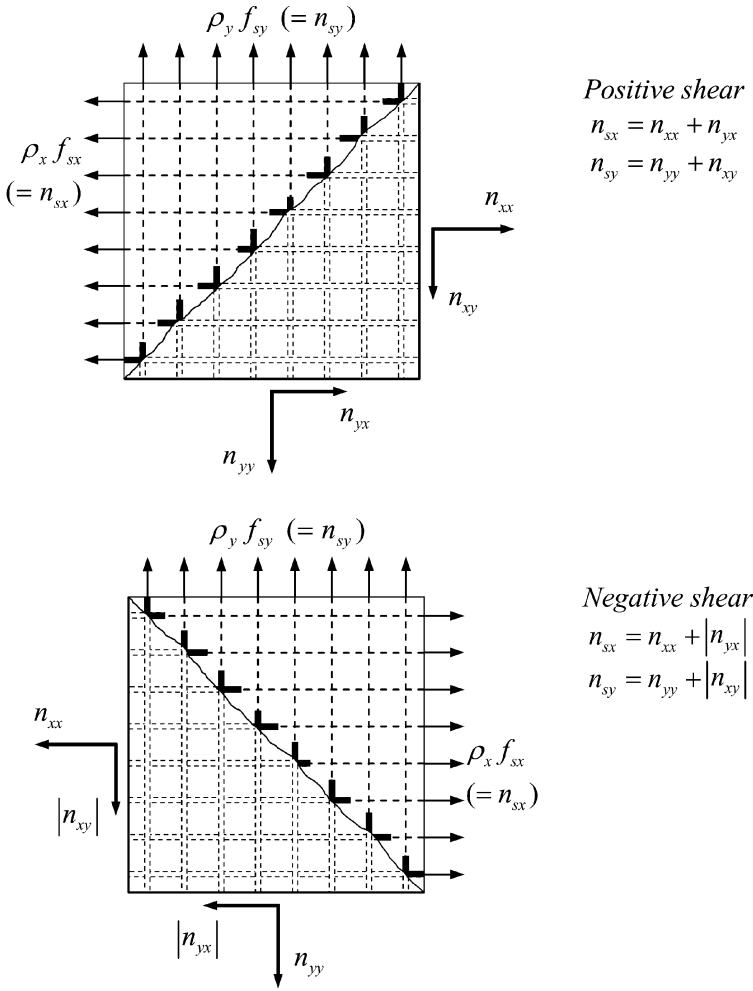


**Figure 11.15** Determination of the reinforcement forces  $n_{sx}$  and  $n_{sy}$ .

bottom part of Figure 11.15. The concrete struts are now in the direction of the other diagonal. It is a consequence of the assumed cracked state that compressive stresses occur in the concrete. A shear membrane stress  $\sigma$  causes a compressive stress of  $2\sigma$  in the concrete struts, as is seen in Figure 11.16. This follows from the equilibrium of a strut of width  $s\sqrt{2}$  if  $s$  is the spacing between the reinforcement bars.

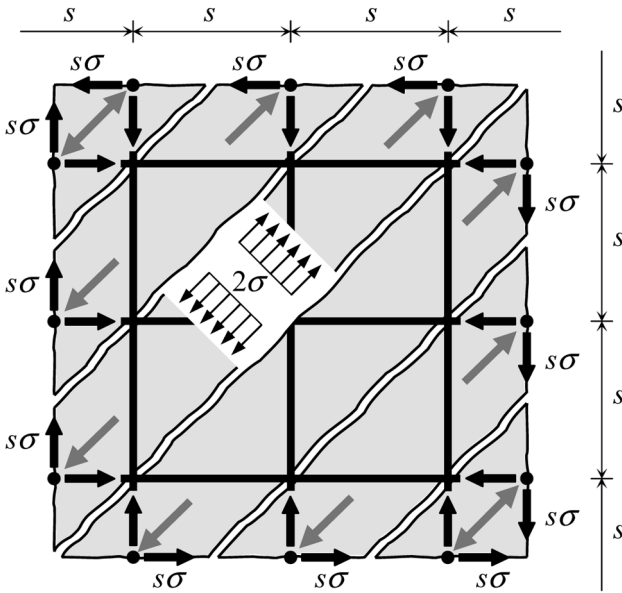


**Figure 11.16** Cracked concrete, tensioned reinforcement, diagonal compressive struts.

## 11.7 Message of the Chapter

- Lateral contraction due to Poisson's ratio can be responsible for unexpected local increases of stress.
- FE analyses show stress concentrations where classic beam calculations suppose smooth stress distributions. Sometimes they reveal omissions in design.
- If the theory of elasticity predicts a singular stress, refinement of mesh in the FE analysis will lead to ever increasing stress values. No convergence will be obtained.
- Linear-elastic FE analysis can be a help to structural engineers who like to use strut-and-tie models in detailing reinforced concrete.

- Re-entrant corners are singular stress spots in membrane structures. Here, averaging of discontinuous stress values must be done with care.
- The structural engineer can account for severe cracking in a linear-elastic FE analysis by judiciously reducing Young's modulus in cracked regions. An example is a tall wall with a row of rectangular openings. This structure can alternatively be handled as a frame.